© 2016. Published by The Company of Biologists Ltd | Journal of Cell Science (2016) 129, 3878-3891 doi:10.1242/jcs.183137

RESEARCH ARTICLE

Characterization of prion protein function by focal neurite stimulation

Ladan Amin[1], Xuan T. A. Nguyen[1], Irene Giulia Rolle[1], Elisa D'Este[2], Gabriele Giachin[1,*], Thanh Hoa Tran[1], Vladka Čurin Šerbec[3], Dan Cojoc[4,‡] and Giuseppe Legname[1,‡]

ABSTRACT

The cellular prion protein (PrP^C), encoded by the *PRNP* gene, is a ubiquitous glycoprotein, which is highly expressed in the brain. This protein, mainly known for its role in neurodegenerative diseases, is involved in several physiological processes including neurite outgrowth. By using a novel focal stimulation technique, we explored the potential function of PrP^C, in its soluble form, as a signaling molecule. Thus, soluble recombinant prion proteins (recPrP) encapsulated in micro-vesicles were released by photolysis near the hippocampal growth cones. Local stimulation of wild-type growth cones with full-length recPrP induced neurite outgrowth and rapid growth cone turning towards the source. This effect was shown to be concentration dependent. Notably, PrP^C-knockout growth cones were insensitive to recPrP stimulation, but this property was rescued in PrP-knockout growth cones expressing GFP–PrP. Taken together, our findings indicate that recPrP functions as a signaling molecule, and that its homophilic interaction with membrane-anchored PrP^C might promote neurite outgrowth and facilitate growth cone guidance.

KEY WORDS: Prion protein, Neurite outgrowth, Growth cone guidance and signaling, Local delivery

INTRODUCTION

Directional motion of neurites to synaptic targets is a complex process controlled by a combination of several mechanisms (Kolodkin and Tessier-Lavigne, 2011). Growth cones, found at the tip of neurites, are the most motile structures of developing neurons and enable them to explore the environment in search of guidance cues necessary for precise wiring of the neural network (Dent and Gertler, 2003; Vitriol and Zheng, 2012). The cellular form of the prion protein (PrP^C; SwissProt ID P04156) is a membrane-anchored glycoprotein that is present in almost all cell types and is particularly abundant in neurons. Its predominant expression in synapses, growth cones and other extending process tips in cultured cells (Santuccione et al., 2005) suggests that it might play a key role in synaptic signaling and growth cone navigation.

[1]Department of Neuroscience, Laboratory of Prion Biology, Scuola Internazionale Superiore di Studi Avanzati (SISSA), I-34136 Trieste, Italy. [2]Max Planck Institute for Biophysical Chemistry, D-37077 Göttingen, Germany. [3]Department for Production of Diagnostic Reagents and Research, Blood Transfusion Centre of Slovenia, 1000 Ljubljana, Slovenia. [4]Optical Manipulation (OM)-Lab, Institute of Materials (IOM), National Research Council (CNR), I-34149 Trieste, Italy.
*Present address: European Synchrotron Radiation Facility (ESRF), Structural Biology Group, 71 Avenue des Martyrs – CS 40220, Grenoble F-38043 Cedex 09, France.

‡Authors for correspondence (cojoc@iom.cnr.it; legname@sissa.it)

L.A., 0000-0001-6388-8869; D.C., 0000-0003-2243-4478

Received 4 November 2015; Accepted 16 August 2016

It is now widely accepted that PrP^C can convert into misfolded isoforms, known as prions, responsible for the neurodegeneration observed in prion diseases (Prusiner et al., 1998). Moreover, recent evidence indicates that PrP^C might also mediate the neurotoxicity effect of amyloid beta (Aβ) oligomers that are associated with Alzheimer's disease (Lauren et al., 2009). Although the pathogenic properties of PrP^C have been intensely studied, its physiological role remains unclear. So far PrP^C has been associated with several cellular processes, including cell signaling (Linden et al., 2008), survival (Aguzzi et al., 2008) and adhesion (Malaga-Trillo et al., 2009) as well as neuritogenesis (Loubet et al., 2012; Steele et al., 2006), differentiation (Hajj et al., 2007; Kanaani et al., 2005) and brain metal homeostasis (Pushie et al., 2011). PrP^C interacts with different surface or transmembrane molecules, including laminin, laminin receptor precursor and neural cell adhesion molecule (NCAM)-family members, contributing to many of the above mentioned processes (Linden et al., 2008). For instance, cis- and trans-interaction of PrP^C with NCAM on the surface of mouse neurons has been shown to result in recruitment of NCAM to lipid rafts and activation of Fyn and to promote neurite outgrowth (Santuccione et al., 2005).

Additional reports have indicated that PrP^C can be secreted from the cell membrane and released to the extracellular space through distinct mechanisms (Martins et al., 2010). Therefore, PrP^C can interact with neighboring cells either in a soluble form or in exosomes, which are released by cells upon fusion of multivesicular bodies with the cell surface (Fevrier et al., 2004). In this context, experimental evidence has revealed that the treatment of hippocampal neurons with recombinant PrP (recPrP) enhances the development of neuronal polarity and formation of neuronal networks after 24–48 h (Kanaani et al., 2005). However, this approach exposed cells to constant molecular concentrations and, hence, did not allow focal stimulation of specific neuronal compartments. In the present study, we performed experiments in conditions mimicking the interaction between a single growth cones and a gradient of soluble recPrP, taking advantage of a recently developed technique for local delivery of molecules encapsulated in phospholipid vesicles (Pinato et al., 2012; Sun and Chiu, 2003, 2005). Our results reveal a new molecular function of recPrP as a guidance molecule, which might interact with like molecules (homophilic interaction) on the neighboring cells to regulate signal transduction. These findings highlight a key physiological role for PrP^C during developmental, as well as in adult life.

RESULTS

recPrP induces neurite outgrowth and rapid growth cone turning

Although prion protein has been suggested to contribute to neurite outgrowth (Kanaani et al., 2005; Loubet et al., 2012), its role in neurite navigation has not yet been investigated. To test whether

Journal of Cell Science

Journal of Cell Science (2016) 129, 3878-3891 doi:10.1242/jcs.183137

recPrP molecules can directly influence neuronal growth cone steering, we used an *in vitro* assay for axon guidance based on a local stimulation technique (Pinato et al., 2012). This technique employs infrared (IR) laser tweezers to trap and position a lipid vesicle carrying guidance molecules in the proximity of the cell. The molecules are then released by vesicle photolysis mediated by a pulse from a second ultraviolet (UV) laser.

Here, we employed recPrP molecules. Despite the lack of posttranslational modifications [e.g. N-glycosylation at residues N180 and N196 and a glycosylphosphatidylinositol (GPI) anchor], full-length recPrP is structurally equivalent to brain-derived PrP^C (Hornemann et al., 2004); thus, it represents a valuable model for structural and functional studies. Taking into account that UV light might induce protein damage by direct photo-oxidation and radical reactions (Redecke et al., 2009), we investigated the structural consequences of UV and IR radiations on murine recPrP. Protein samples were exposed to 7 min UV (355 nm) followed by 2 h of IR irradiation (1064 nm) to mimic the irradiation conditions during the stimulation experiment, based on the characteristics of the lasers (energy and beam size). Circular dichroism spectra of each sample were recorded before and immediately after laser irradiation (Fig. S1). We found that in both conditions (UV and UV+IR irradiated samples), the spectra of the protein remain unaffected, indicating that neither UV nor IR radiation alter recPrP structural features in our experimental assays.

After vesicle photolysis, molecules freely diffuse in all directions and only a fraction of them reaches the growth cone membrane. The number of molecules reaching the leading edge depends on the starting concentration of the molecules inside the vesicle, distance between the growth cones and vesicle, and the diffusion coefficient of molecules (Pinato et al., 2012). Assuming the concentration inside the vesicle and the size of vesicle are known, we calculated the spatial and temporal distribution of the concentration of the molecules at the growth cones (see Materials and Methods). The numerical example in Materials and Methods, using a set of parameters consistent with the real experiments, shows that a spatial gradient of ∼2 nM/µm can be delivered to the growth cones from the microvesicle.

In our experimental assay, 4 µM of recPrP were encapsulated in lipid vesicles with a diameter that varied between 1 and 5 µm. Vesicles were introduced to the cell culture medium, and a single vesicle was trapped and positioned by an IR laser tweezer near an exploring hippocampal growth cone (Fig. 1A,B; Materials and Methods). Using a short UV laser pulse, the membrane of the vesicle was then broken and the protein content was released and allowed to reach the growth cone by free diffusion.

With this assay, the outgrowth and turning of neurite can be measured in response to a defined stimulus of recPrP over a short time period (Fig. 1A–D). Following the release of recPrP (4 µM), we observed a rapid neurite outgrowth and a significant turning towards the source of the stimuli (Fig. 1E,F; Movie 1). Rapid growth cones motions started at 1–2 min after vesicle breaking, and within 600 s the neurite outgrowth was enhanced 2–3-fold compared to control (Fig. 1F, maximum neurite growth within entire duration of experiment reached to 6.73±0.80 µm; mean±s.e.m.). Quantification of the turning angle revealed that neurites had a significant bias toward the source (Fig. 1E, blue rose distribution). Control vesicles, filled with phosphate-buffered saline (PBS), were positioned and photolysed in proximity of exploring growth cones (Fig. 1A; Movie 2). Following vesicle photolysis, the growth cones continued the spontaneous navigation without significant changes in growth or direction (Fig. 1E,F, maximum neurite elongation in this case reached to 2.88±0.36 µm). Remarkably, the neurite outgrowth induced by recPrP was significantly correlated with the turning angle (Fig. 1G; correlation coefficient $R=-0.64$, $P<0.05$), but no significant correlation was observed in the control. This confirms that local recPrP stimulation was concomitant with simultaneous fast neurite growth and growth cones turning toward the protein source.

Indeed, these experiments strengthen the evidence that PrP^C is involved in neurite outgrowth and differentiation but also suggest a putative physiological function for soluble PrP as a guidance molecule for mouse hippocampal growth cones that promotes neurite outgrowth and influences the directional motion of neurites.

We next wondered whether changing the concentration of recPrP reaching the growth cones could influence its navigation. Therefore, growth cones were stimulated with different concentrations of recPrP. As expected, at low concentration (0.5 µM), the maximum growth was similar to control and no significant turning was observed. When increasing the concentration of recPrP from 1 to 4 µM, both neurite elongation and growth cones turning toward the source increased significantly (Fig. 2). However, these effects were diminished by increasing the concentration to 6 µM and the opposite effects were observed at 15 µM (Fig. 2). Taken together, these data suggest that recPrP influences growth cone navigation in a dose-dependent manner: outgrowth and turning are stimulated progressively only when the concentration increases up to a certain value. For higher concentrations, the outgrowth is decreased or even becomes retraction (at concentrations 3–4-fold higher than the threshold). A low concentration of recPrP at the plasma membrane is sufficient to initiate signaling, whereas increased recPrP concentration might interfere with signaling cascades or activate different pathway leading to growth cone retraction and collapse.

Full-length PrP role in growth cone navigation

Next, we examined whether the stimulatory effect of recPrP was dependent on the full-length molecule or whether a similar effect could be reproduced by truncated forms of PrP. To ensure that the recombinant proteins were not degraded or cleaved by proteases during the incubation time in neuronal medium before or during the experiments, we analyzed the integrity of each PrP fragment at different time points (0, 20, 40, 60 and 120 min) after addition to the medium by western blotting. We found that all fragments of PrP used in this study remained stable for the entire duration of the experiments (Fig. 3A,B).

Local delivery of the N-terminal (23–90) domain of recPrP (up to 8 µM) slightly increased the average growth in comparison to control condition but the result did not reach statistical significance (Fig. 3D–F). Surprisingly, local delivery of the C-terminal (89–231) domain (4 µM) caused an opposing effect on growth cone dynamics and, in some cases, growth cones retracted completely (Fig. 3C). Quantification of the turning angle indicated that none of the fragments was able to induce growth cone orientation toward the source (Fig. 3D,F). Notably, The mixture of 4 µM of recPrP(23–90) and 4 µM recPrP(89–231) had a very similar effect to what was observed after local delivery of the C-terminal domain (89–231); this is, no significant growth or turn was detected (Fig. 3E,F). We also performed experiments using 4 µM recPrP(23–120) and the mixture of recPrP(23–120) and recPrP(89–231). We found that although recPrP(23–120) slightly enhanced the maximum growth with respect to the control condition, the mixture of this fragment and recPrP(89–231) is not functionally active (Fig. 3E,F). These results are consistent with the associated pro- and anti-apoptotic functions of the C- and N-terminal domain of PrP^C (Martins et al., 2010), confirming that the growth-promoting function of recPrP is more pronounced in the presence of the full-length protein.

Journal of Cell Science

Journal of Cell Science (2016) 129, 3878-3891 doi:10.1242/jcs.183137

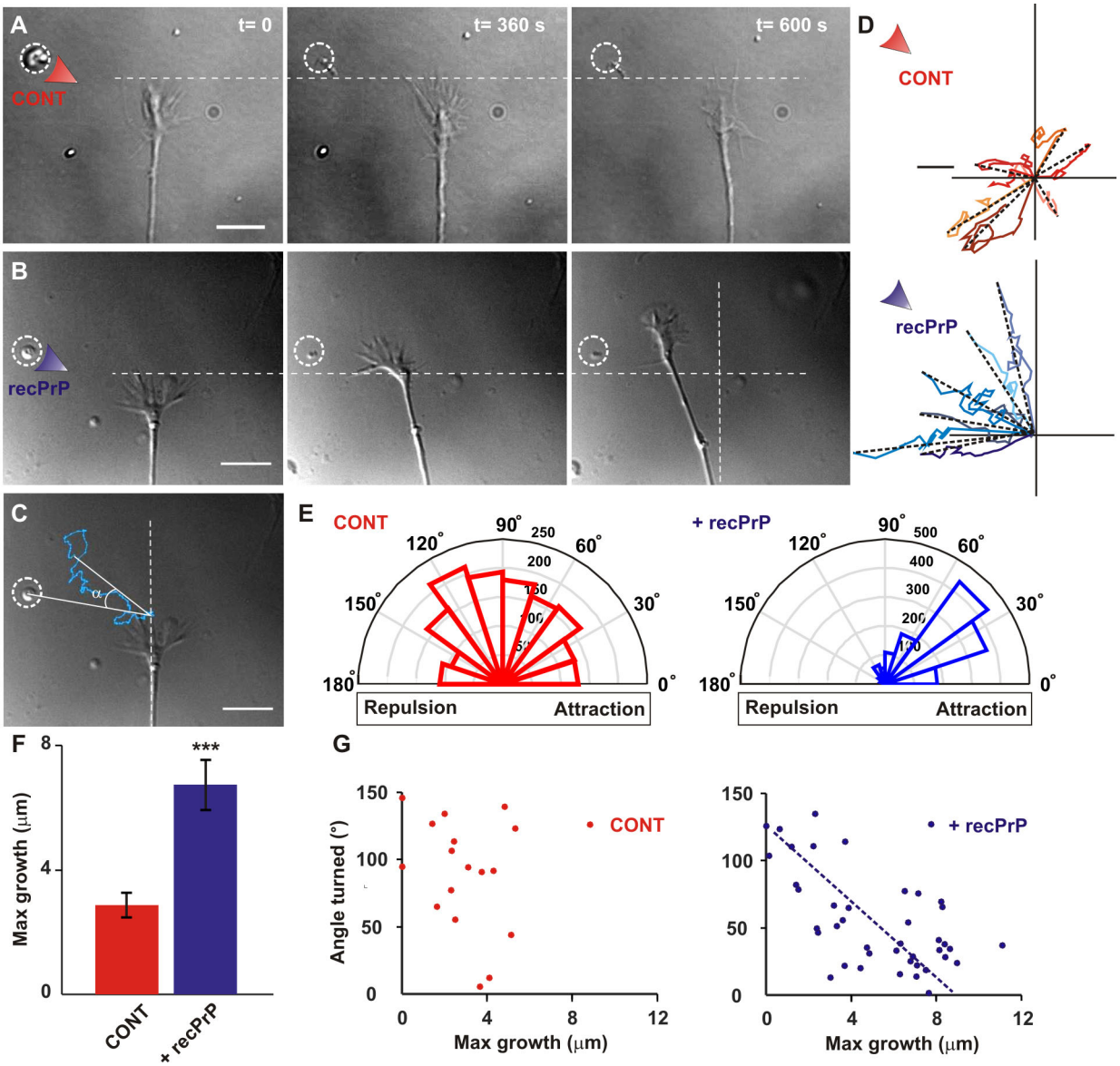

Fig. 1. Local delivery of PrP induces fast neurite outgrowth and causes turning towards the source. (A,B) DIC images of growth cone dynamics after vesicle (dotted circle) photolysis at t=0 s. Red arrowheads indicate the position of vesicle encapsulating PBS (CONT, A) and 4 µM recPrP (B). After recPrP release, growth cones clearly grew faster and turned towards the vesicle. (C) Definition of the growth and turning angle, α. The growth was derived from the position of the leading edge in successive frames, whereas the turning angle was defined as the angle between the direction of neurite extension and vesicle position for each frame. The blue line represents the detected leading edge position at different times. Scale bars: 8 µm. (D) Superimposed trajectories of neurite extension after PBS (up) and recPrP (down) stimulations for six growth cones. Trajectories were normalized to the distance between the initial position of growth cones and vesicle position. Scale bar: 2 µm. Dotted lines indicate the principal direction of growth. (E) Distributions of turning angle (absolute value) for control and recPrP (n=22 and 49 growth cones respectively) showing large angular distribution for control and a much narrower distribution for stimulation with recPrP. (F) The value of maximum neurite outgrowth, defined with respect to t=0 s. recPrP stimulation enhanced neurite outgrowth up to threefold. Data represent mean±s.e.m. ***P<0.001 (Student's t-test). (G) Scatterplot of the maximum neurite outgrowth versus turning angle for control (left) and after recPrP release (right). The dashed line represents the linear interpolation of the data points.

Previous studies have identified the biochemical similarities between the flexible N-terminal domain of PrP^C and a newly discovered GPI-linked glycoprotein called Shadoo (Sho; also known as SPRN). This protein is also expressed in the adult brain. Furthermore, it has been suggested that Sho exhibits PrP-like protective properties (Premzl et al., 2003). Therefore, we examined the role of this protein on neurite outgrowth and growth cone navigation. Local delivery of 4 µM Sho did not influence the growth cone navigation (Fig. S2).

Membrane-anchored PrP^C acts as a signaling receptor

We then investigated how neurons respond to extracellular recPrP stimuli and where the primary site of this interaction could be. Previous studies have suggested that GPI-anchored PrP^C itself could be one of the candidates for mediating the effect of PrP (Malaga-Trillo et al., 2009). To test this hypothesis, PrP-knockout mouse ($Prnp^{0/0}$) models were used. As a preliminary control of the neuronal cultures used in this study, endogenous PrP^C expression was evaluated in PrP wild-type (wt) and knockout neurons at 24 and

Journal of Cell Science

Journal of Cell Science (2016) 129, 3878-3891 doi:10.1242/jcs.183137

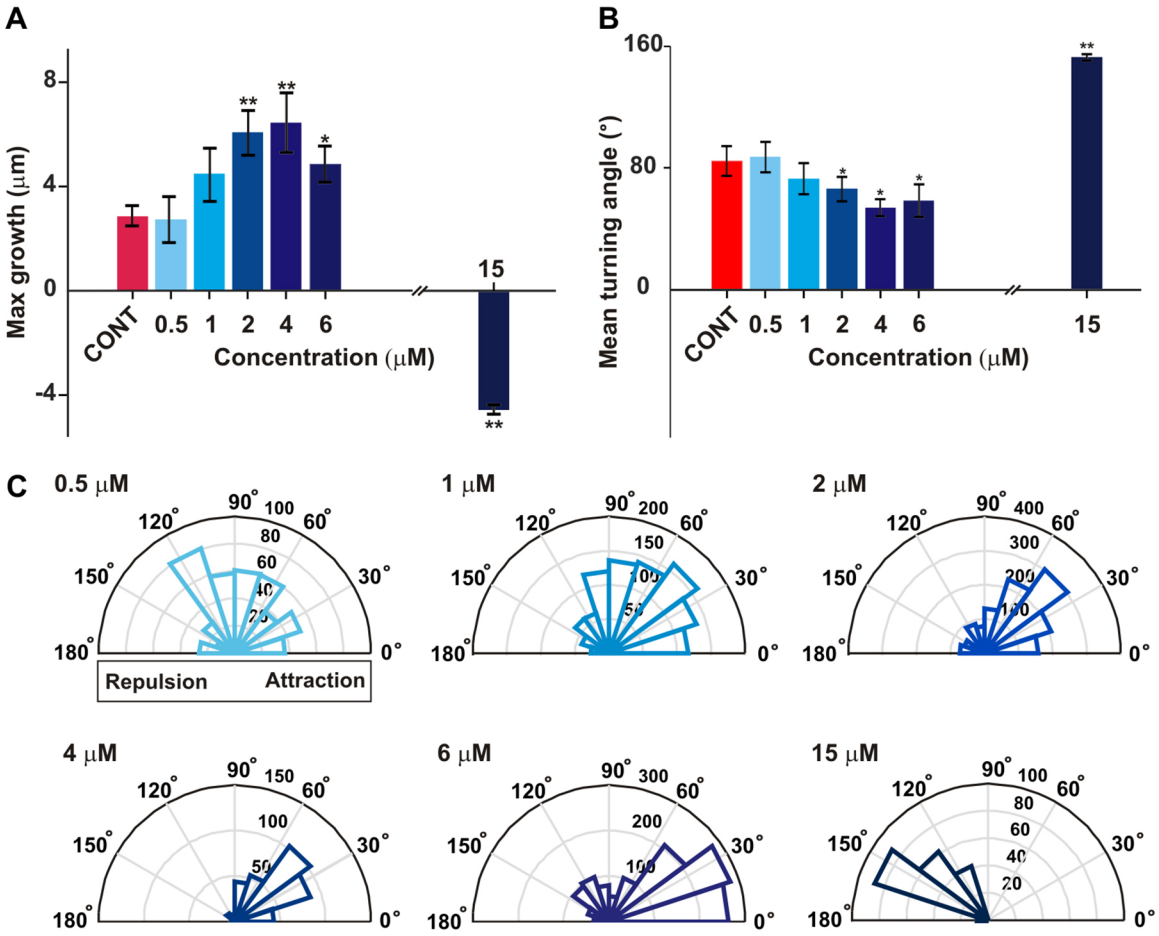

Fig. 2. The growth cone response to recPrP stimulation depends on the recPrP concentration. (A) Color-coded bars indicate maximum neurite outgrowth with respect to concentration of recPrP inside the vesicle. Data represent mean±s.e.m. $P<0.05$, one-way ANOVA; *$P<0.05$, **$P<0.01$ for *t*-test with Holm-Bonferroni correction for multiple comparison. (B) Mean turning angle with respect to concentration of recPrP inside the vesicle. Data represent circular mean±s.e.m. $P<0.001$, one-way ANOVA for circular data; *$P<0.05$, **$P<0.01$, Watson–Williams test with Holm-Bonferroni correction for multiple comparison. $n>10$ growth cones for A and B. (C) Color-coded rose distributions indicate the change of growth cone direction as a function of concentration. By increasing the concentration of recPrP inside the vesicles, maximum neurite elongation increased substantially and growth cones turn towards the source in a dose-dependent manner. At very high concentrations, growth cones retracted completely (dark blue bar).

48 h after plating the neurons. PrP^C was expressed in wt neurons with its normal glycosylation pattern (Fig. 4A), presenting three isoforms (unglycosylated, mono-glycosylated and di-glycosylated protein). After peptide-N-glycosidase F (PNGase F; an amidase that cleaves oligosaccharides from N-linked glycoproteins) digestion, PrP^C is mainly deglycosylated. PrP^C-ablated neurons do not show PrP expression as expected.

Comparing growth cone dynamics in wt and *Prnp*$^{0/0}$ neurons, we found that PrP-null growth cones were insensitive to recPrP release (Fig. 4B,C; Movie 3), undergoing repetitive cycles of protrusions and retractions, without any significant growth or change in direction (Fig. 4D,E). Although PrP-null growth cones were growing at a slower rate in comparison to wt neurons (Fig. 4C), they were able to respond to other guidance cues such as netrin-1. When growth cones were exposed to netrin-1 stimulation, within a few minutes growth cones clearly turned toward the vesicle position (Fig. 4F,G; Movie 4). These results suggested that these two signaling events followed two different signaling pathways. In all species, the attractive effects of netrin are meditated by well-documented receptors of the deleted in colorectal carcinomas (DCC) family (Moore et al., 2007) whereas our experimental data on the *Prnp*$^{0/0}$ mice model predicted that the potential function of recPrP as a signaling molecule requires membrane-anchored PrP^C to exert its functions. To further clarify this issue, *Prnp*$^{0/0}$ neurons were transfected with GFP–PrP constructs and examined after local stimulations with 4 μM recPrP (Fig. 4H,I). GFP-tagged PrP would be expected to have the same glycosylation pattern as the endogenous protein, and previous studies have shown that GFP-tagged PrP is correctly localized and functionally active in the brains of transgenic mice (Barmada et al., 2004). Moreover, it has been shown that GFP–PrP expressed in prion-infected cells has the same localization as wt PrP after Proteinase K digestion (Bian et al., 2006). Notably, in our assay, GFP–PrP-expressing growth cones acquired the ability to respond to recPrP stimuli and neurite outgrowth enhancement was rescued compared to control (Fig. 4J).

To check the accuracy and reliability of our experimental data, we compared data from different mouse strains – FVB and C57 black6 (for wt), and FVB and Zurich I (for *Prnp*$^{0/0}$) mice (Fig. S3). The recPrP effects were identical, indicating that recPrP stimulation enhanced neurite outgrowth in a similar manner in both mouse strains. Neither significant growth nor growth cone turning was observed in experiments using *Prnp*$^{0/0}$ neurons originating from both FVB and Zurich I mice.

Considering the relevance of homophilic interaction between PrP^C molecules in our experimental assay, we then asked which

Journal of Cell Science (2016) 129, 3878-3891 doi:10.1242/jcs.183137

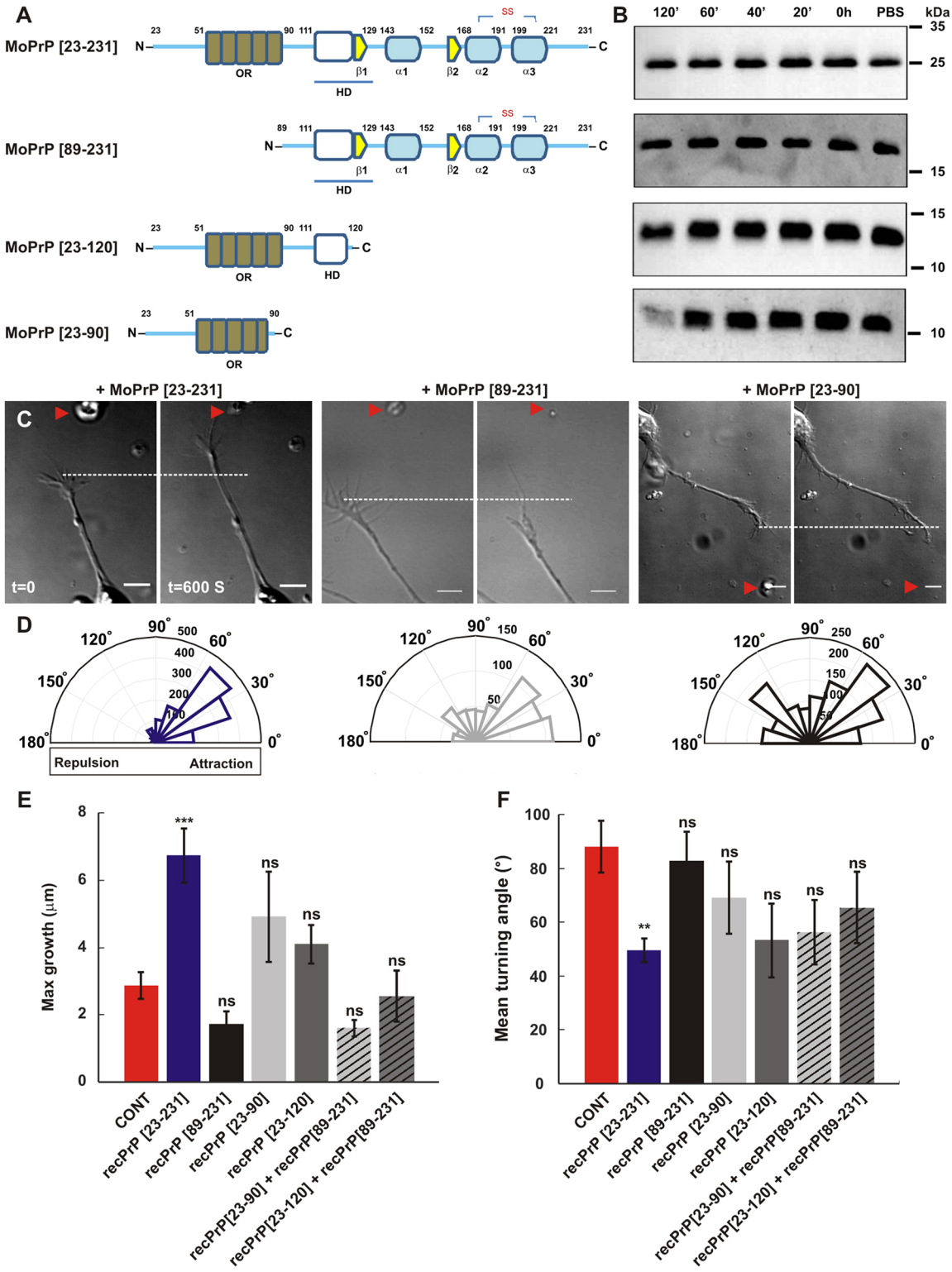

Fig. 3. Full-length PrP had a more active role in growth cones navigation. (A) Mouse full-length PrP (MoPrP) and its different domains proteins as used in this study. OR, octarepeats; HD, hydrophobic domain. (B) Western blot analysis shows that different PrP fragments (in A) remain stable after incubation in neuron medium (NBM) supplemented with FBS. Different incubation times were used: 0, 20, 40, 60 and 120 minutes. Protein in PBS was used as a positive control. W226 (binding epitope: 145–155) was used to detect full-length recPrP(23–231) and the PrP C-terminal fragment (89–231) but EB8 (binding epitope: 26–34) was used for N-terminal fragment detection (residues 23–120 and 23–90). (C) DIC images of a growth cone before and after vesicle photolysis. Red arrowheads indicate the position of vesicle encapsulating 4 µM of full-length recPrP, N-terminal recPrP(23–90) and C-terminal recPrP(89–231). The dotted line is used as an indication of the start position. Scale bar: 8 µm. (D) Angle distributions when full-length, C-terminal and N-terminal PrP fragments were delivered to growth cones. (E) Maximum neurite outgrowth in control conditions and in presence of different fragments and their mixture. Data represent mean±s.e.m. $P<0.001$, one-way ANOVA; ***$P<0.001$, *t*-test with Holm-Bonferroni correction for multiple comparison. (F) Mean turning angle. Data represent circular mean±s.e.m. $P<0.05$, one-way ANOVA for circular data; **$P<0.01$, Watson–Williams test with Holm-Bonferroni correction for multiple comparison; ns, not significant. $n>10$ growth cones for E and F.

Journal of Cell Science

Journal of Cell Science (2016) 129, 3878-3891 doi:10.1242/jcs.183137

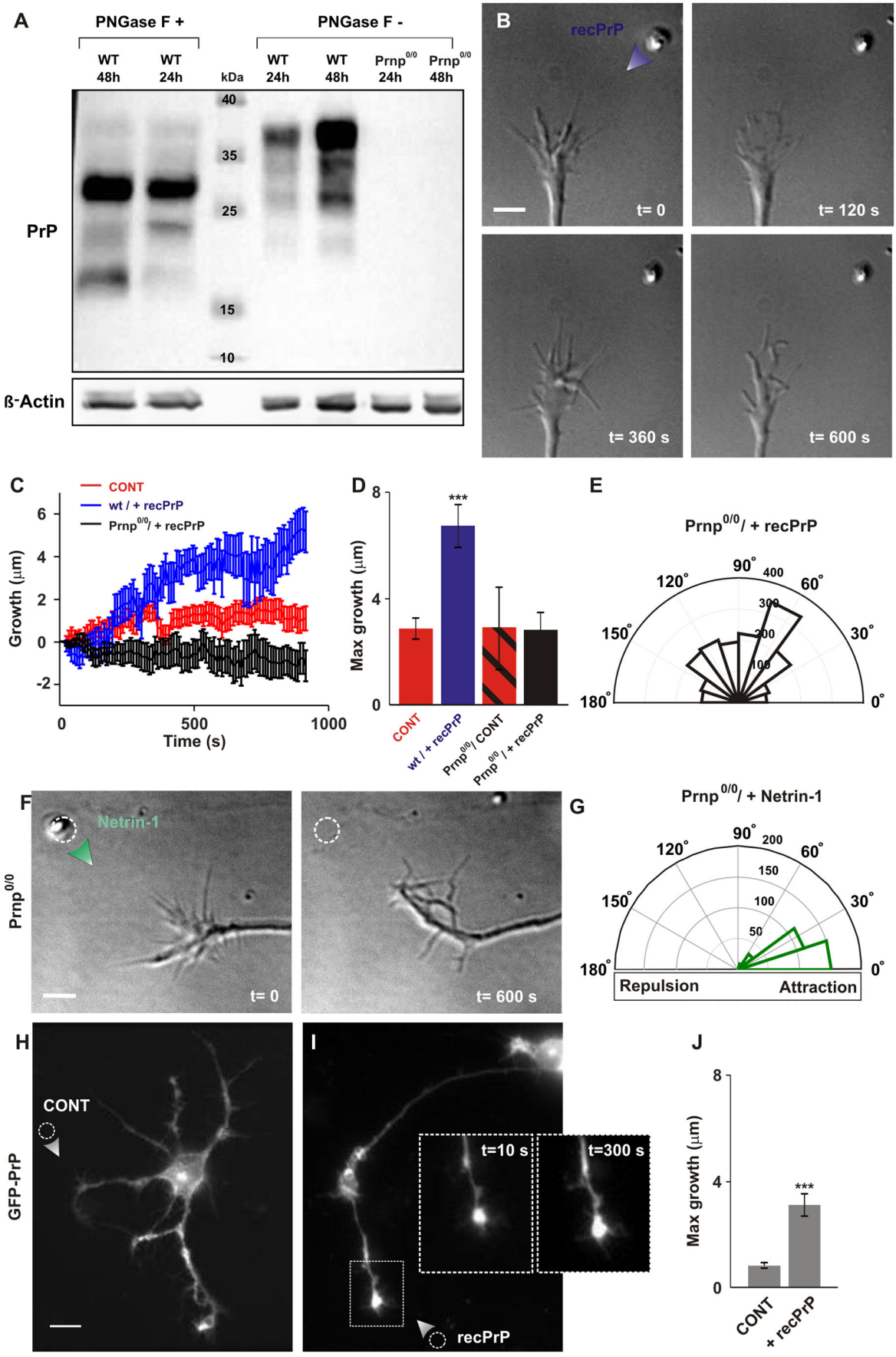

Fig. 4. See next page for legend.

Journal of Cell Science

Journal of Cell Science (2016) 129, 3878-3891 doi:10.1242/jcs.183137

Fig. 4. recPrP requires expression of PrP^C on the membrane to exert its functions. (A) PrP^C expression in primary hippocampal neurons at 24 and 48 h after dissection. Western blot analysis using anti-PrP W226 antibody was performed. PrP^C expression was evaluated in wt neurons before (right) and after (left) PNGase F treatment. *Prnp*$^{0/0}$ neurons were used as negative control. β-actin was used as loading control. (B) DIC images of a *Prnp*$^{0/0}$ growth cone after recPrP stimulation. No significant growth was observed after vesicle photolysis. Scale bar: 5 µm. (C) Time evolution of neurite outgrowth after recPrP release in *Prnp*$^{0/0}$ growth cones superimposed with collected data from wt growth cones. Results are mean±s.e.m.; *n*=49, 22 and 25 for blue, red and black curves, respectively. (D) Bars indicate the value of the maximum neurite outgrowth in control conditions and after 4 µM recPrP stimulation in wt and *Prnp*$^{0/0}$ growth cones. *n*>10 growth cones. Data represent mean±s.e.m. ***P<0.001, Holm–Bonferroni correction for multiple comparison. (E) Distribution of angle after local delivery of recPrP to *Prnp*$^{0/0}$ growth cones (*n*=25 growth cones). (F) DIC images of a *Prnp*$^{0/0}$ growth cone after local delivery (dotted circle) of netrin-1. After vesicle breaking, growth cones clearly turned toward the source. Scale bar: 4 µm. (G) As in E, but with vesicle encapsulating netrin-1. (H,I) Fluorescence images of GFP–PrP-expressing neurons immediately after local stimulation with PBS (H) and 4 µM recPrP (I). Arrowheads indicate the position of the vesicles. Scale bar: 8 µm. Insets indicate the time-lapse images of growth cones marked in I. (J) Bars indicate the value of maximum neurite outgrowth after local stimulation of GFP–PrP-expressing growth cones [*n*=9 and *n*=10 growth cones for control (CONT) and recPrP-stimulated conditions, respectively]. Restoring PrP to the growth cone membrane rescued neurite outgrowth enhancement.

region of PrP^C is mediating this interaction. To address this question, PrP^C was probed with three different monoclonal antibodies (mAbs) to test their ability to bind distinct epitopes situated in the distal region of both the PrP^C N- and C- terminus. The localization of PrP^C was investigated by immunostaining with W226 (Petsch et al., 2011; binding epitope: 145–155), SAF34 (Perrier et al., 2004; binding epitope: 59–89) and EB8 (Didonna et al., 2015; binding epitope: 26–34). All three mAbs recognized the PrP^C in wt mouse hippocampal neuronal culture, showing similar staining patterns (Fig. 5A). After 30 min of incubation with mAbs (1 µg/ml), they were washed out and recPrP was delivered locally to growth cones. Interestingly, the growth-promoting effect of recPrP was completely abolished after treatment with W226 and SAF34 (Fig. 5B,C), whereas EB8 was not able to block the effect of recPrP at the concentration used. These data suggest that the homophilic interaction of recPrP and PrP^C is necessary to provide distinct signaling events and that defined epitopes of PrP^C might regulate this homophilic interaction.

PrP^C mediates multiple signaling pathways

We showed that murine recPrP might interact with PrP^C as a putative receptor or part of receptor complex to exert its function. However, it remains largely unclear how recPrP stimuli are transduced in the cell interior. To gain preliminary insight into the intracellular signaling mechanisms involved in recPrP-mediated neurite outgrowth on mouse hippocampal culture, a panel of kinase inhibitors was tested for its ability to inhibit the effect of recPrP on neurite elongation (Fig. 6). Src family kinases, including Fyn, are known to have roles in mediating both prion neurotoxicity and PrP-mediated cell signaling. In addition to the Src family kinases, extracellular regulated kinase 1 and 2 (ERK1/2, also known as MAPK3 and MAPK1, respectively) and phosphatidylinositol 3-kinase (PI3K) can regulate a broad range of cellular process including cell differentiation, adhesion and migration (reviewed in Ochs and Málaga-Trillo, 2014).

In this set of experiments, neurons were incubated with different inhibitors for 30 min and then 4 µM recPrP (stripped blue bars in Fig. 6) or PBS (stripped red bars in Fig. 6) was delivered to the growth cones. As summarized in Fig. 6, PP2 (1 µM), a selective inhibitor of the Src kinase, blocked the enhancing and guiding

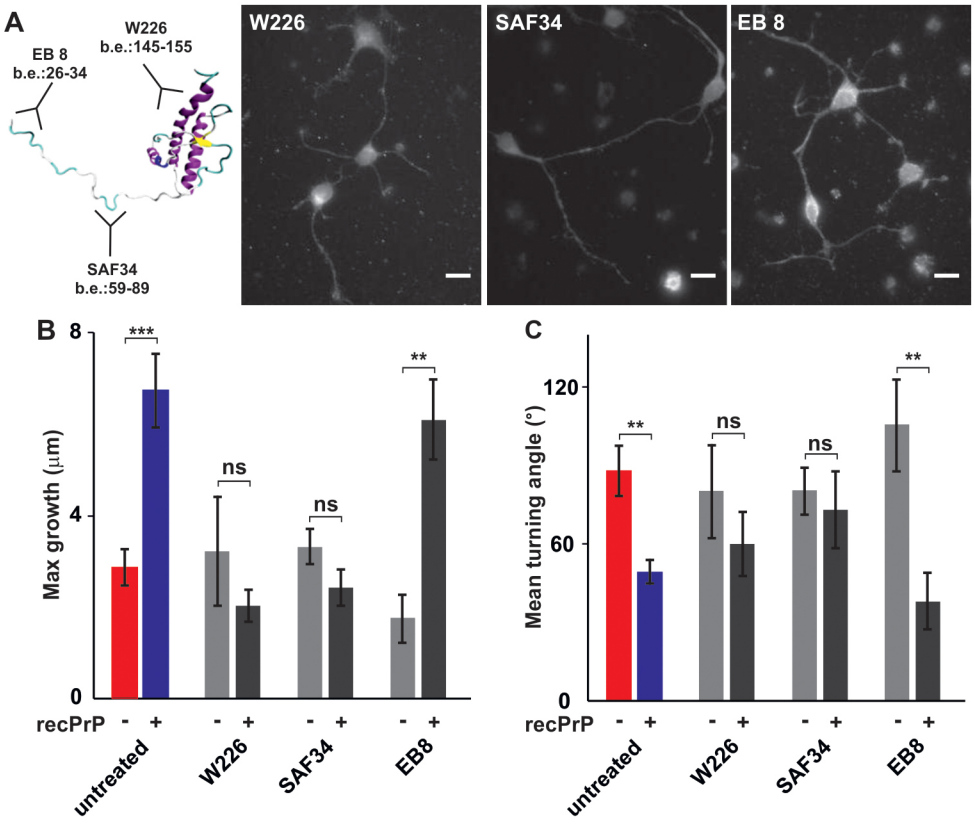

Fig. 5. mAbs against PrP^C block growth promoting effect of recPrP. (A) Hippocampal neurons were fixed and immunostained with the three mAbs. All the antibodies showed a similar pattern. Scale bars: 10 µm. Cartoon indicates three-dimensional structure of mouse PrP^C and the binding epitopes (b.e.) of the mAbs. (B,C) Maximum neurite outgrowth (B) and mean turning angle (C) in control conditions and in the presence of 4 µM recPrP. Cells were pre-treated with different mAbs against PrP^C (W226, EB8 and SAF34; 1 µg/ml). In the presence of W226 and SAF34 no significant growth and turn was observed, whereas EB8 did not block the growth-promoting effect of recPrP. Data in B represent mean±s.e.m. P<0.001, two-way ANOVA; **P<0.01, ***P<0.001, *t*-test with Holm–Bonferroni correction for multiple comparison. (C) Mean turning angle. Data represent circular mean±s.e.m. P<0.001, two-way ANOVA for circular data; **P<0.01, Watson–Williams test with Holm–Bonferroni correction for multiple comparison; ns, not significant.

Journal of Cell Science (2016) 129, 3878-3891 doi:10.1242/jcs.183137

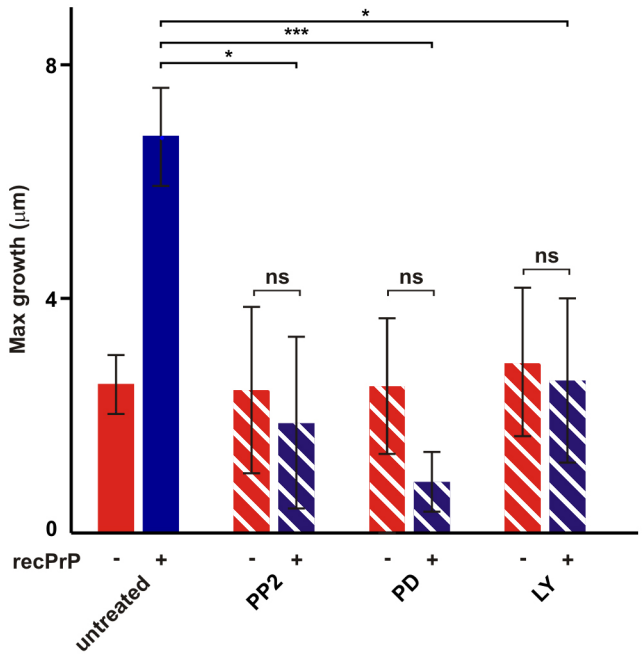

Fig. 6. Effect of kinase inhibitors on PrP-induced neurite outgrowth. Quantification of the maximum neurite outgrowth in control conditions (red bars) and after stimulation by 4 µM recPrP (blue bars). Solid bars indicate untreated experiments and stripped bars indicate 30 min incubation with different kinase inhibitors. Treatment with 1 µM PP2 (a selective inhibitor of the Src family kinase; n=12 growth cones), 50 µM PD98059 (PD, inhibitor of the ERK1/2 pathway; n=11 growth cones) and 20 µM LY294002 (LY, an inhibitor of PI3K; n=10 growth cones) block the effect of recPrP indicating that multiple signaling pathways were involved in transduction of recPrP-mediated signals. Data represent mean±s.e.m. P<0.001, two-way ANOVA; *P<0.05, ***P<0.001, t-test with Holm–Bonferroni correction for multiple comparison; ns, not significant.

effects of recPrP by more than 70%; this is in agreement with previous studies that have shown that Src kinase is an important kinase involved in PrP^C-mediated intracellular signaling and its role in neurite outgrowth (Chen et al., 2003; Kanaani et al., 2005; Ochs and Málaga-Trillo, 2014). Furthermore, to investigate whether other activation of other kinases, including ERK1/2 and PI3K, are necessary for recPrP-mediated neurite outgrowth we tested PD98059 (50 µM), and inhibitor of the MEK (MAP2K) and ERK pathway, and LY294002 (20 µM), an inhibitor of PI3K. Collected data indicate that inhibition of ERK1/2 and PI3K abolishes the effect of recPrP on neurite elongation.

Therefore, in our experimental assay, neurite outgrowth and turning triggered by recPrP in cultured mouse hippocampal neurons require the activity of the Src kinase family, including Fyn, and ERK1/2 and PI3K activation. Thus, these data indicate that multiple signaling pathways were involved in transduction of recPrP-mediated signals.

recPrP and PrP^C interaction promote neurite outgrowth and guidance through PrP^C–NCAM interaction

PrP^C is anchored to the outer leaflet of the plasma membrane through a GPI anchor; therefore, it is unlikely to physically associate with cytosolic molecules. Nevertheless, a number of transmembrane and intracellular molecules are known to functionally cooperate with PrP^C to transduce signals into the cell interior (Linden et al., 2008). Among them, NCAM-family proteins have attracted interest because both PrP^C and NCAM have been implicated in signaling cascades involving the Src kinase family and because Src is also involved in NCAM-driven neurite outgrowth (Santuccione et al., 2005; Schmitt-Ulms et al., 2001).

First, we investigated the role of NCAM (SwissProt ID P13591) in growth cone motility by using mAb against NCAM. Surprisingly, the growth-promoting effect of recPrP was abolished after treatment with (1 µg/ml) mAb against NCAM (Fig. 7F). These data suggest that NCAM might be involved in signal transduction.

To further investigate the role of NCAM in our assay, we analyzed the colocalization of PrP^C and NCAM in cultured mouse hippocampal neurons in control conditions (Fig. 7A) and in the presence of 2 µM recPrP (bulk treatment) (Fig. 7B) using stimulated emission depletion (STED) nanoscopy (Klar et al., 2000). Low colocalization was measured between PrP^C and NCAM in control culture, whereas after recPrP treatment colocalization increased significantly (Fig. 7B,E). In control conditions, both molecules showed uniform distribution along neurites (Fig. 7A). In contrast, in recPrP-treated cultures, clusters of NCAM signal overlapped with PrP^C (Fig. 7B) suggesting that recPrP treatment can affect NCAM clustering in the plasma membrane.

To exclude the contribution of recPrP from observed colocalization, we pre-treated the cells with EB8 antibody against PrP. After 30 min of incubation, unbounded antibodies were washed out and cultures were treated in bulk with 2 µM of recPrP for 2 h. We found a slightly lower colocalization (not a significant difference, P>0.4) than for the case when the cells were exposed directly to recPrP (Fig. 7C,E). Notably, this value was also significantly different from the control, suggesting that recPrP treatment recruits NCAM to lipid rafts, and would increase the association between NCAM and PrP^C. We then asked whether increased association between PrP^C and NCAM is specific to recPrP treatment or whether another growth-promoting factor can cause a similar effect on the distribution of NCAM and/or PrP^C. To address this issue, samples were treated in bulk with 1 µM nerve growth factor (NGF) and examined with STED nanoscopy (Fig. 7D,F). Surprisingly, we also observed higher colocalization between PrP^C and NCAM in NGF-treated samples, suggesting that recruitment of NCAM to lipid rafts is a generic property of neurite outgrowth stimulation.

Higher colocalization of NCAM and PrP^C in recPrP-treated cultures suggested that these proteins might form a complex in lipid rafts, activate Src and downstream members of the Src kinase pathway, and in turn trigger the growth. This is in line with previous studies in cultured mouse hippocampal neurons (Santuccione et al., 2005) where PrP^C was found to directly interact with NCAM through cis or trans interaction, stabilizing NCAM within lipid rafts, and thereby stimulating neurite outgrowth.

DISCUSSION

In the present study, we undertook experiments in conditions that mimic the interaction between a single growth cone and locally released recPrP molecules, unraveling the long-awaited putative physiological function for soluble full-length PrP as a signaling molecule and GPI-anchored PrP^C as its receptor. Previous studies have indicated that PrP^C can be secreted from the cell membrane and released to the extracellular space through distinct mechanisms (Martins et al., 2010). The GPI anchor can be removed by post-translational modification (Borchelt et al., 1993; Harris et al., 1993) or cleaved by phospholipase C (Parkin et al., 2004). Moreover, PrP^C can reach the extracellular space in exosomes, which are released by cells upon fusion of multivesicular bodies with the plasma membrane (Fevrier et al., 2004). Therefore, PrP^C might interact

Journal of Cell Science (2016) 129, 3878-3891 doi:10.1242/jcs.183137

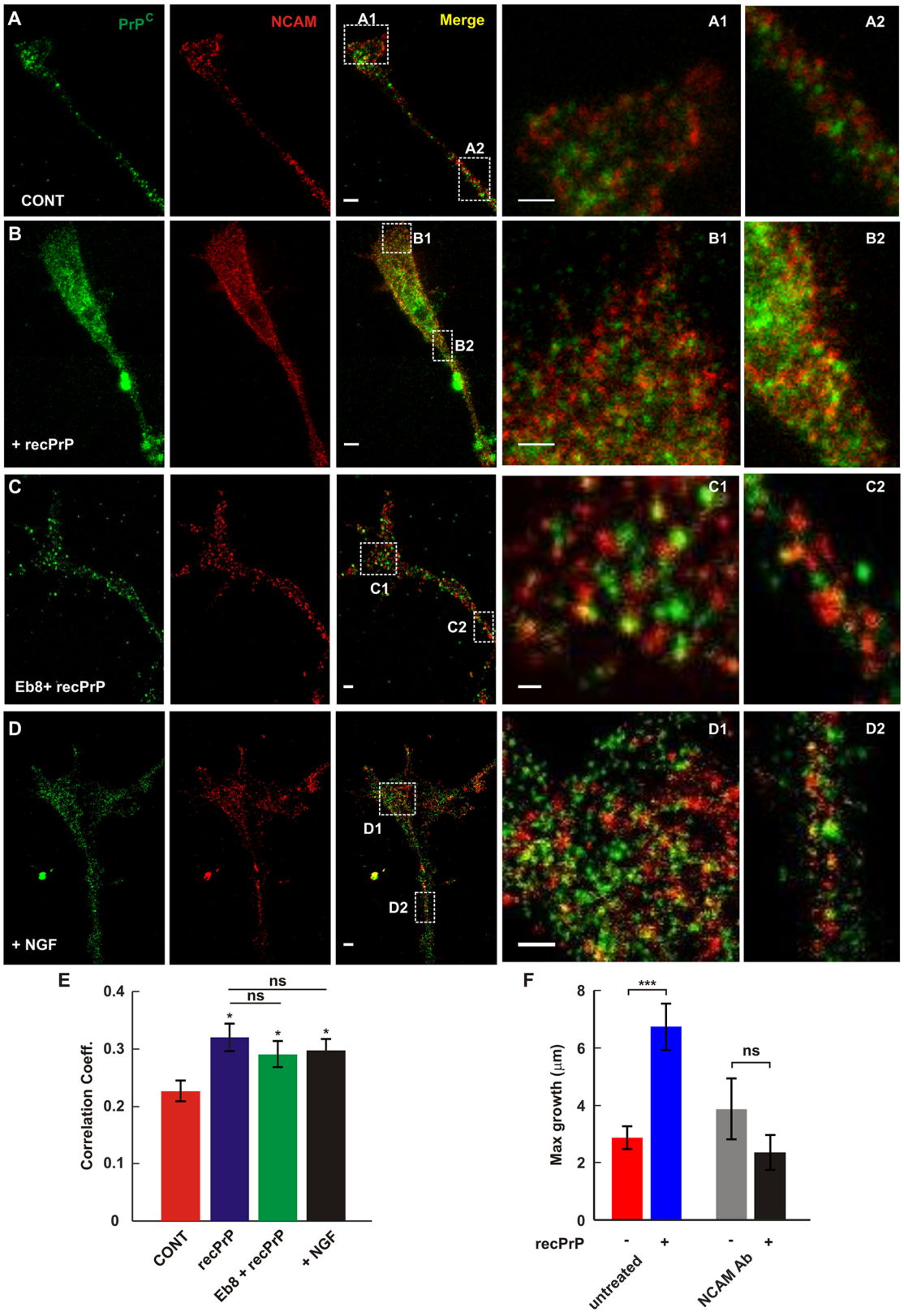

Fig. 7. recPrP treatment increase the colocalization between PrP and NCAM. (A) STED images of growth cones stained for PrP and NCAM, and the merge of the two stainings in control conditions. Scale bar: 500 nm. (A1,A2) High-resolution images of areas indicated in A. Scale bar: 250 nm. (B) As in A, but neurons were incubated in bulk with 2 µM recPrP (2 h). (C) As in A, but in this case cells were pre-treated with mAb against PrP (1 µg/ml of EB8 for 0.5 h) and then incubated with 2 µM recPrP (2 h). (D) As in A, but neurons were treated in bulk with 1 µM NGF for 2 h. (E) Mean correlation coefficients comparing the colocalization between PrP and NCAM in different conditions. $P<0.05$, one-way ANOVA. (F) Maximum neurite outgrowth in control condition and in presence of recPrP. Cells were pre-treated with mAbs against NCAM (1 µg/ml). In the presence of mAb, no significant growth was observed. Data represent mean±s.e.m. $P<0.001$, two-way ANOVA; *$P<0.05$, ***$P<0.001$, *t*-test with Holm–Bonferroni correction for multiple comparison; ns, not significant.

Journal of Cell Science

Journal of Cell Science (2016) 129, 3878-3891 doi:10.1242/jcs.183137

with neighboring cells in a soluble form. Our methodology enabled experimental conditions to examine and visualize the function of soluble PrP as a guidance molecule.

Comparing neurite navigation in wt and *Prnp*$^{0/0}$ growth cones, we found that *Prnp*$^{0/0}$ growth cones were insensitive to recPrP stimulation but they were still able to respond to other biochemical cues such as netrin-1. These results strongly suggest that physiologically active PrP^{C} on the membrane is required to mediate recPrP stimulation and activate downstream signaling events. There is evidence supporting the notion that PrP^{C} functions as a part of cell surface platform to interact selectively with various sets of ligands and transmembrane modules, mediating distinct signaling events, which in turn modulate specific physiological processes or behavior (Aguzzi et al., 2008; Linden et al., 2008).

Moreover, we show that local accumulation of recPrP at wt growth cone leading edges requires the activation of multiple intracellular tyrosine kinases including the Src-family kinases and other kinases such as ERK1/2 and PI3K to initiate any motile behavior. There is a general agreement that PrP-mediated signaling in neurons can trigger activation of Src-related kinases, such as Fyn (Chen et al., 2003; Ochs and Málaga-Trillo, 2014). More importantly, the non-receptor Src-related kinases are able to regulate a broad range of cellular process in physiology and disease. For instance Src-related kinases are known to regulate cell adhesion through direct phosphorylation of p120 and β-catenins (Lilien and Balsamo, 2005). Thus, PrP^{C} signaling might modulate cell adhesion and consequently reorganize actin cytoskeleton dynamics through the activation of Src-related kinases. Furthermore, consistent with a previous investigation (Chen et al., 2003), our experimental data support that the ERK1/2 and PI3K are involved in recPrP signal transduction. PI3K is involved in various cellular functions, including proliferation, cell migration and axon guidance (Cantley, 2002; Chang et al., 2006). It has been reported that PI3K activity mediates growth cones attractive turning responses to guidance cues such as NGF, BDNF and netrin-1 (Li et al., 2005).

The observation that full-length recPrP is more active in inducing physiological responses poses intriguing issues about the role of N- and C-terminal domains for PrP^{C} function: although the C-terminus moiety possesses well-defined secondary and tertiary structures, the N-terminus is unstructured. These segments are often considered to be independent and not to interact with each other (Zahn et al., 2000). However, recent studies have attributed a significant role to the N-terminus in driving tertiary structure contacts with the C-terminus, and this structural proximity appears to be mediated by metal ions (i.e. copper and zinc ions) binding the octarepeats domain located in the N-terminal moiety (Spevacek et al., 2013; Thakur et al., 2011). Interestingly, we found that treatments of wt mouse hippocampal neurons with SAF34 and W226 mAbs – targeting the N- and C-terminus, respectively – completely abolished the growth promoting effect induced by recPrP. By contrast, EB8 mAb – which binds a region adjacent to the octarepeats domain – does not show any inhibitory effect. These results seem to support a model whereby PrP^{C} exerts its growth-promoting function through a mechanism mediated by the interplay between the flexible octarepeat region and the structured domain.

PrP^{C} might undergo multiple processing by disintegrins. These cleavages occur within the putative toxic domain comprising residues 106–126. The processing is carried out by members of the a disintegrin and metalloproteinase (ADAM) enzyme family, including ADAM8, ADAM10 and ADAM17. ADAM8 cleaves PrP^{C} at residue 109 or 116, whereas ADAM10 and ADAM17 cleave at residue 119. ADAM10 can also process the C-terminal domain of PrP at position 227. This complex post-translational process leads to production of different fragments displaying various physiological functions.

The first such processing carried out by ADAM8, which cleaves at residue 109, yields two moieties denoted N1 and C1, for the N-terminal and C-terminal domains, respectively. These two fragments have been shown to possess opposing biological activities (Chen et al., 1995; McDonald and Millhauser, 2014). In our experiments, we used either PrP(23–89) or PrP(23–120) to test whether the N-terminal domain had growth cones guidance properties. Although some limited effect was observed, the results were not statistically significant.

Taken together, we propose a defined mechanism underlying the interaction of recPrP with growth cones. Local accumulation of recPrP at wt growth cone sites and its homophilic interactions with membrane PrP^{C} activate Src-related kinase (including Fyn), along with their downstream signaling pathways, to transduce the recPrP signal into the cell interior. Focal adhesion molecules and the actin cytoskeleton are the major targets of these signaling cascades at the growth cone periphery. Therefore, local stimulation with recPrP might activate new adhesion formation at the leading edge nearest to the guidance cue and promote actin remodeling at the growth cone periphery, which in turn facilitates neurite outgrowth and mediates the attractive guidance response. Most likely, the association of PrP^{C} is not the sole player in transduction of recPrP-mediated signals and other cell surface proteins, such as NCAM, are implicated in activation of signaling cascade by forming complexes on the membrane. This mechanism is consistent with a role of PrP^{C} in the modulation of cell adhesion through signaling (Linden et al., 2008), and supports previous evidence in a zebrafish study showing that PrP^{C} itself promotes Ca^{+2}-independent homophilic cell adhesion and suggesting a functional link between PrP^{C} and E-cadherin to modulate Ca^{+2}-dependent cell adhesion (Malaga-Trillo et al., 2009). Other studies have reported that overexpression of PrP^{C} modulates focal adhesion dynamics by regulating Src and FAK phosphorylation both in mammals and *Drosophila* (Schrock et al., 2009).

In summary, our study shows a defined molecular function of PrP^{C} in inducing neurite outgrowth and rapid growth cone turning, which might provide new insights into understanding of its physiological roles during developmental stage and adult life. Further investigations might establish whether PrP^{C} has a potential role in affecting axon regeneration in the adult nervous system.

MATERIALS AND METHODS

Antibodies

Three different mouse mAbs with the ability to bind to distinct epitopes of PrP^{C} were used in local delivery, immunoblotting and immunocytochemical experiments. W226 (Petsch et al., 2011) binds to C-terminal domain of PrP^{C} (epitope: 145–155), whereas SAF34 (Perrier et al., 2004) and EB8 (Didonna et al., 2015; Snajder et al., 2012) bind to N-terminal domain of PrP^{C} (epitope: 59–89 and 26–34, respectively). Anti-NCAM antibodies (AB5032 from Millipore) were used in local delivery and immunocytochemical experiments.

Cell culture and transfection

Postnatal day (P)1–P2 FVB wt and PrP-deficient (*Prnp*$^{0/0}$) mice were killed by decapitation in accordance with the guidelines of the Italian Animal Welfare Act. Details of the neuron preparation can be found in Amin et al. (2013). Briefly, after decapitation, hippocampi were dissected, cut into slices and washed twice with the dissection medium [9.52 mg/ml Hank's modified (Ca^{2+} and Mg^{2+} free), 350 mg/ml $NaHCO_3$, 2.83 mg/ml Hepes, 6 mg/ml D-glucose, 200 mM kinurenic acid, 25 mM APV, 300 mg/ml BSA and 1.44 mg/ml $MgSO_4$]. The enzymatic dissociation was performed by

treating the slices with 5 mg/ml trypsin (Sigma-Aldrich, St Louis, MO) and 0.75 mg/ml DNase I (Sigma-Aldrich) in digestion medium (8 mg/ml NaCl, 0.37 mg/ml KCl, 0.99 mg/ml Na_2HPO_4, 6 mg/ml Hepes, 0.35 mg/ml $NaHCO_3$, 200 mM kinurenic acid, 25 mM APV; 5 min, room temperature). Then, trypsin was neutralized by addition of 1 mg/ml trypsin inhibitor (Sigma-Aldrich) in the dissection medium for 10 min on ice. After washing in the dissection medium, mechanical dissociation was performed in the same dissection medium with 0.6 mg/ml DNase I by performing ∼50 passages through a Gilson P1000 tip. The cell suspension was then centrifuged at 100 ***g*** for 5 min, and the pellet re-suspended in the culture medium. Finally, hippocampal neurons were plated on coverslips coated with 50 µg/ml poly-L-ornithine (Sigma-Aldrich). The hippocampal neuronal culture was incubated (5% CO_2, 37°C) in minimum essential medium with Earle's salts and Glutamax I with 10% fetal bovine serum (FBS) and 2.5 µg/ml gentamycin (all from Invitrogen, Life Technologies, Gaithersburg, MD), 6 mg/ml D-glucose, 3.6 mg/ml Hepes, 0.1 mg/ml apo-transferrin, 30 µg/ml insulin, 0.1 µg/ml biotin, 1.5 µg/ml vitamin B12 (all from Sigma-Aldrich). In order to find isolated growth cones, we performed local delivery experiments 24–48 h after plating the neurons. In STED experiments 2-day-old *in vitro* cultures were treated in bulk with 2 µM recPrP or 1 µM NGF for 2 h and then cells were fixed and stained for NCAM and PrP^C. The concentration of recPrP was chosen in a way to have maximum effect on growth cone motion.

Cells were transfected with pcDNA-EGFP-PrP using Lipofectamine 3000 for Primary cells (Life Technologies, Grand Island, NY) according to the manufacturer's instructions. The open reading frame encoding for the pre-protein mouse PrP(1–254) was amplified by PCR from genomic murine DNA and cloned in pcDNA3.1(-) vector (Invitrogen). To generate the construct of GFP–PrP targeted to the membrane, the sequence coding for GFP from the plasmid pEGFP-N1 (Clontech) was amplified and inserted downstream of N-terminal PrP signal peptide sequence (residues 1–23) by a restriction-free cloning method (van den Ent and Lowe, 2006; RF method). The plasmid pcDNA-GFP-PrP was verified by DNA sequencing, isolated and purified by Maxiprep kits (Qiagen) prior to transfection.

Protein production

The full-length mouse PrP(23–231), the truncated mouse PrP(23–120) and the truncated mouse PrP(89–231) were cloned, expressed and purified according to our previous protocols (Giachin et al., 2014), whereas the peptide corresponding to the truncated mouse PrP(23–90), N-terminal acetylated and C-terminal amidated, was chemically synthesized (Chematek Inc, Milano, Italy). All the mouse PrP polypeptides were prepared in PBS buffer. Sho protein was a gift from Prof. David Westaway (University of Alberta; Edmonton, AB, Canada).

Western blot analysis

Primary hippocampal neurons were lysed in lysis buffer (50 mM Tris-HCl pH 7.5, 150 mM NaCl, 0.5% CHAPS, 1 mM EDTA and 10% glycerol) supplemented with protease inhibitor mixture (Roche), and processed for western blot detection. Neuronal samples and recombinant mouse PrP, prepared as described above, were analyzed by standard immunoblotting procedures. Samples were loaded onto SDS-PAGE gels and transferred to nitrocellulose membranes (GE Healthcare). After blocking in 5% non-fat dried milk in Tris-buffered saline supplemented with 0.1%; Tween-20 (TBS-T) for 1 h at room temperature, membranes were incubated overnight at 4°C with primary antibody diluted in blocking solution. Incubation for 1 h at room temperature with secondary antibody followed. Western blot image acquisition was performed using the ECL detection kit and the Alliance 4.7 software (UVITECH, Cambridge). The antibodies used were as follows: mouse monoclonal anti-PrP (W226, 1:1000), mouse monoclonal anti-PrP (EB8, 1:1000), horseradish peroxidase (HRP)-conjugated mouse monoclonal anti-β-Actin (A3854, Sigma, 1:10,000). HRP-conjugated secondary antibodies were obtained from DAKO and were diluted 1:2000 in blocking solution.

Vesicle preparation

The following composition of lipid mixture was used for vesicle preparation: cholesterol, 9 µmol; L-α-phosphatidylcholine, 63 µmol; and stearylamine, 18 µmol (Sigma-Aldrich). The lipid solution was prepared at the concentration of 10 mg/ml in chloroform-methanol (2:1, v/v). The solution obtained was then saturated with nitrogen and stored at −20°C. Vesicles with a diameter of 1–5 µm were obtained by using the lipid film rehydration method (Hub et al., 1982; Pinato et al., 2012). In this method, lipid solution is dried in vacuum conditions for 24 h and then the lipid film is rehydrated with solution containing the desired concentration of recPrP. Sucrose (100 mM) was also included in the hydration solution to allow better vesicle washing and to improve vesicle trapping. After overnight incubation, vesicles were gently centrifuged (1783 ***g*** for 3 min) and rinsed three times with PBS to wash the external solution. Final vesicle solution was then administered to the cell cultures. Single vesicles were subsequently identified, trapped and positioned at the location of interest.

Estimation of the spatial and temporal distribution of the concentration of recPrP at the growth cones

To perform this simulation, we used the point source approximation for the vesicle (Sun and Chiu, 2005) and the following equation that describes three-dimensional free diffusion from a point source:

$$C(r,t) = 2 \times \frac{C}{(4\pi Dt)^{3/2}} e^{-(r^2/Dt)},$$

where C is the initial concentration in the vesicle, D the diffusion coefficient and C(r,t) the concentration in a point at distance r from the vesicle, at time t. The concentration versus time curves for three points positioned at distances r, 1.25r and 1.5r are represented in the top inset of the Fig. 8A, indicating a steep temporal gradient. The concentration at a distance r from the vesicle reaches a maximum after a few seconds and then decreases fast to a value which is maintained almost constant in time after t=10 s. From the concentration curves represented for different distances, we notice also the spatial gradient and the fact that the spatial gradient tends to vanish after ∼10 s from vesicle photolysis.

However when an obstacle, such as the cell membrane, is reached, the molecules might stop their free diffusion, bind and accumulate on the membrane. Assuming that all the molecules reaching the membrane bind to it, we calculate the spatial and temporal distribution of the cumulative concentration CC(r,t) by summing C(r,t) values:

$$CC(r,t) = \sum_t \sum_r C(r,t).$$

As a numerical example, we consider a vesicle of 4 µm diameter with an initial concentration inside the vesicle C_0=4 µM, the diffusion coefficient of the encapsulated molecules as D=40 $\mu m^2/s$, and the distance r ranging from 10 to 50 µm measured from the vesicle and t from 0 to 5 min. The spatio-temporal distribution of the concentration is shown in Fig. 8B, showing that for a given distance the concentration increases fast immediately after the photolysis and tends to a constant value after ∼2 min, whereas a significant spatial gradient is maintained at a constant level in time after ∼3 min. The concentration isolines are represented in Fig. 8C. Notice that after 3 min the concentration decreases from 90 nM to 20 nM for a distance range of ∼40 µm. The vesicle is typically positioned at 10–20 µm from the leading edge of the neurite, creating a spatial gradient of molecules concentration of about 2 nM/µm at the growth cones, which promotes the outgrowth and guidance mechanisms.

Optical setup

The optical manipulation setup was developed starting from an inverted microscope (Nikon Eclipse TE-2000-E, Japan) equipped with phase-contrast imaging and epi-fluorescence. The microscope was completed by installing custom IR optical tweezers and a UV laser dissection system (MMI-cellCut Plus, Switzerland). Briefly, the IR laser beam (1064 nm, continuous wave) was collimated and coupled to the optical path of the UV laser beam (355 nm, 0.6-ns pulsed laser). Both beams were directed into the microscope lens (Nikon 60×, NA 1.25) by a dichroic mounted above the fluorescence cube (Pinato et al., 2011). The sample chamber containing the differentiating neurons and the vesicles was placed on the motorized microscope stage. The temperature of the dish was kept at 37°C by a digital temperature controller

Journal of Cell Science

Journal of Cell Science (2016) 129, 3878-3891 doi:10.1242/jcs.183137

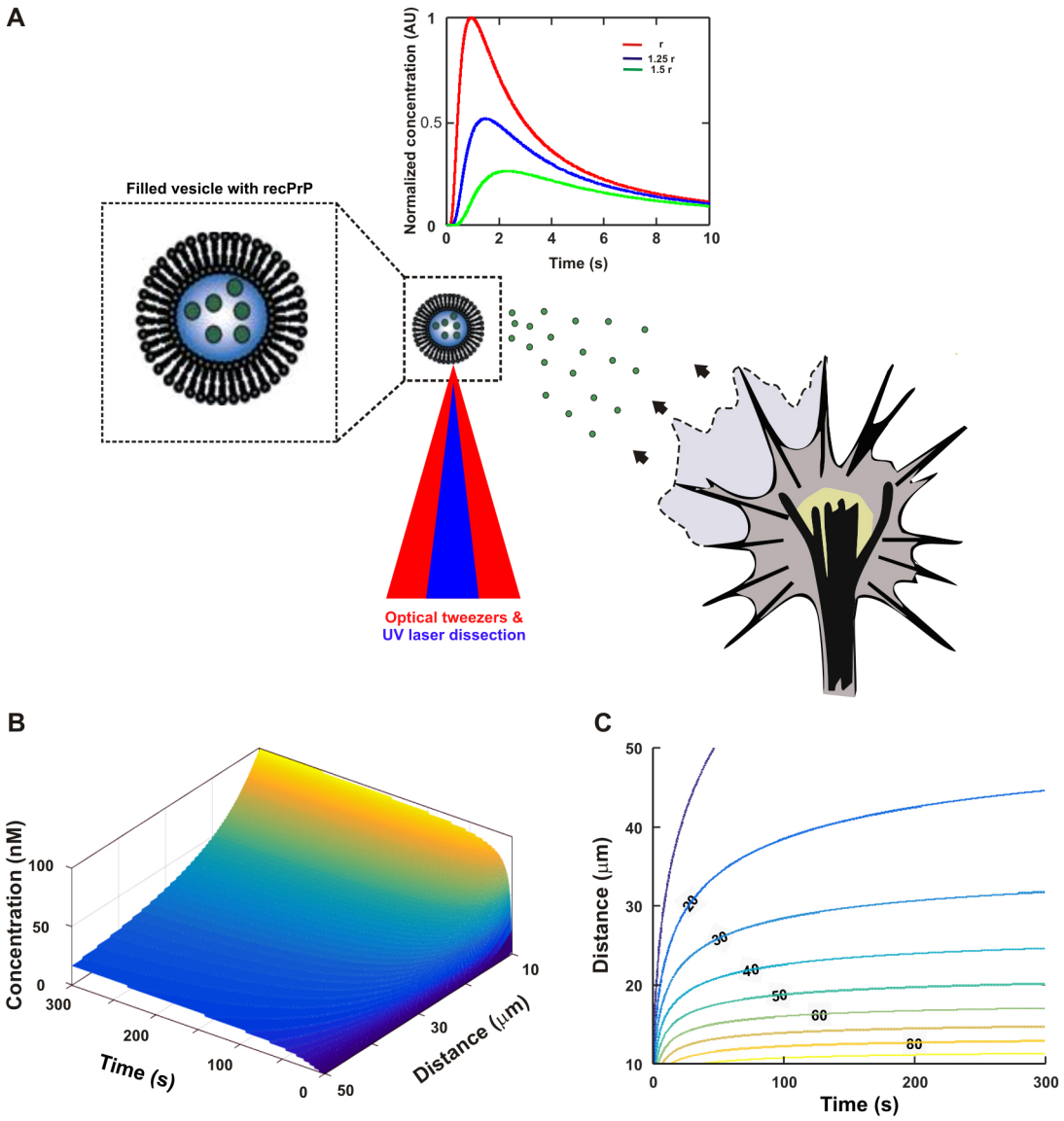

Fig. 8. Schematic representation of the focal stimulation assay. (A) The vesicle, trapped by the IR laser tweezers (red) is positioned near the growth cones and the molecules are released by photolysis of the membrane vesicle with an UV laser pulse (blue). The normalized concentration versus time curves for three points positioned at distances r, 1.25r and 1.5r are represented in the top inset, indicating a steep temporal gradient. The maximum concentrations are reached in 1–2 s and the values decrease from 1 (for r) to 0.5 (1.25 r) and 0.25 (1.5r), also indicating a steep concentration spatial gradient. To generate these curves we have used r=15 μm and D=40 μm^2 /s. (B) The spatio-temporal distribution of the concentration at the growth cones, under the assumption that all the molecules reaching the membrane by free diffusion, bind to it. (C) The concentration isolines (numbers on the isolines indicate concentration in nM).

(PeCon GmbH, Er-back, Germany). During the experiments, the cells were monitored by time-lapse phase contrast imaging using a digital camera (Orca Flash 4.0, Hamamatsu, Japan) at a frame rate of 5 Hz.

Circular dichroism analysis

Circular dichroism spectra of different samples of unexposed, UV and UV+IR-exposed recPrP were recorded using a JASCO J-810 spectropolarimeter. Experiments were performed at room temperature using a 1-mm optical path length quartz cell to obtain spectra in the far-UV region (190 to 260 nm). Protein concentration was 1.2 mg/ml in phosphate buffer (pH 7.4). All spectra reported are the average of at least 10 individual scans.

Immunostaining and imaging

Cells were fixed in 4% paraformaldehyde containing 0.15% picric acid in phosphate-buffered saline (PBS), saturated with 0.1 M glycine, and permeabilized with 0.1% Triton X-100, saturated with 0.5% BSA (all from Sigma-Aldrich) in PBS, and then incubated for 1 h with primary antibodies followed by a 30-min incubation with secondary antibodies conjugated to Alexa Fluor 594 and/or Alexa 488 (all from Invitrogen). All incubations were performed at room temperature (20–22°C). Secondary antibodies used for STED measurements were conjugated to STAR580 or STAR635P (Abberior, Göttingen, Germany).

STED microscopy

Two-color STED microscopy was performed at the NanoBiophotonics Department (Max Plank Institute for Biophysical Chemistry, Göttingen, Germany) on a setup previously described in Gottfert et al. (2013) or on a two-color Abberior STED 775 QUAD Scanning microscope (Abberior Instruments GmbH, Göttingen, Germany) equipped with a 561-nm and 640-nm pulsed excitation lasers, a pulsed 775-nm STED laser, and a 100× oil immersion objective lens (NA 1.4).

Journal of Cell Science

Statistical analyses

Data are shown as mean±s.e.m. and circular statistics were used to compute mean and s.e.m. for angle analysis (MATLAB Circular Statistics Toolbox; Berens, 2009). Statistical significance of the differences between the mean values was evaluated using the *t*-test for outgrowth and colocalization data, and the Watson–Williams test for angle analysis (Berens, 2009). For the cases in which we had multiple comparisons, we used Holm–Bonferroni correction to adjust the *P*-values. An adjusted *P*-value of <0.05 was considered to be statistically significant. For angle data, we used the Watson–Williams test for one-way ANOVA and the Harrison–Kanji test for two-way ANOVA (Berens, 2009).

Acknowledgements

We thank Prof. Stefan W. Hell for allowing and assisting us in the STED experiments run at the Max Planck Institute for Biophysical Chemistry, Göttingen, Germany. We also thank Prof. David Westaway (University of Alberta; Edmonton, AB, Canada) for providing Sho protein, and Prof. Lothar Stitz (Friedrich-Loeffler-Institut, Institute of Immunology, Tuebingen) for providing W226 antibody.

Competing interests

The authors declare no competing or financial interests.

Author contributions

D.C. and G.L. conceived the project. L.A., D.C. and G.L. designed the experiments. D.C. and L.A. developed the local delivery setup and imaging protocols. L.A. performed local delivery and immunofluorescence experiments. L.A., D.C. and G.L. analyzed the data. X.T.A.N., contributed to cell culture. G.G. and T.H.T. contributed to protein production. I.G.R. performed western blot experiments. L.A. and E.D. performed STED experiments and analysis. V.Č.Š. provided the EB8 antibody and supervised the related experiments. L.A., D.C. and G.L. wrote the paper.

Funding

This work was supported by a Fondo per gli Investimenti della Ricerca di Base (FIRB) program project [grant number RBAP11FRE9 to G.L.] from Ministero dell'Istruzione, dell'Università e della Ricerca (MIUR) Italy.

Supplementary information

Supplementary information available online at
http://jcs.biologists.org/lookup/doi/10.1242/jcs.183137.supplemental

References

Aguzzi, A., Baumann, F. and Bremer, J. (2008). The prion's elusive reason for being. *Ann. Rev. Neurosci.* **31**, 439-477.

Amin, L., Ercolini, E., Ban, J. and Torre, V. (2013). Comparison of the force exerted by hippocampal and DRG growth cones. *PLoS ONE* **8**, e73025.

Barmada, S., Piccardo, P., Yamaguchi, K., Ghetti, B. and Harris, D. A. (2004). GFP-tagged prion protein is correctly localized and functionally active in the brains of transgenic mice. *Neurobiol. Dis.* **16**, 527-537.

Berens, P. (2009). CircStat: A MATLAB Toolbox for Circular Statistics. *J. Stat. Soft.* **31**, 10.

Bian, J., Nazor, K. E., Angers, R., Jernigan, M., Seward, T., Centers, A., Green, M. and Telling, G. C. (2006). GFP-tagged PrP supports compromised prion replication in transgenic mice. *Biochem. Biophys. Res. Commun.* **340**, 894-900.

Borchelt, D. R., Rogers, M., Stahl, N., Telling, G. and Prusiner, S. B. (1993). Release of the cellular prion protein from cultured cells after loss of its glycoinositol phospholipid anchor. *Glycobiology* **3**, 319-329.

Cantley, L. C. (2002). The phosphoinositide 3-kinase pathway. *Science* **296**, 1655-1657.

Chang, C., Adler, C. E., Krause, M., Clark, S. G., Gertler, F. B., Tessier-Lavigne, M. and Bargmann, C. I. (2006). MIG-10/lamellipodin and AGE-1/PI3K promote axon guidance and outgrowth in response to slit and netrin. *Curr. Biol.* **16**, 854-862.

Chen, S. G., Teplow, D. B., Parchi, P., Teller, J. K., Gambetti, P. and Autilio-Gambetti, L. (1995). Truncated forms of the human prion protein in normal brain and in prion diseases. *J. Biol. Chem.* **270**, 19173-19180.

Chen, S., Mange, A., Dong, L., Lehmann, S. and Schachner, M. (2003). Prion protein as trans-interacting partner for neurons is involved in neurite outgrowth and neuronal survival. *Mol. Cell. Neurosci.* **22**, 227-233.

Dent, E. W. and Gertler, F. B. (2003). Cytoskeletal dynamics and transport in growth cone motility and axon guidance. *Neuron* **40**, 209-227.

Didonna, A., Venturini, A. C., Hartman, K., Vranac, T., Curin Serbec, V. and Legname, G. (2015). Characterization of four new monoclonal antibodies against the distal N-terminal region of PrP(c). *PeerJ* **3**, e811.

Fevrier, B., Vilette, D., Archer, F., Loew, D., Faigle, W., Vidal, M., Laude, H. and Raposo, G. (2004). Cells release prions in association with exosomes. *Proc. Natl. Acad. Sci. USA* **101**, 9683-9688.

Giachin, G., Narkiewicz, J., Scaini, D., Ngoc, A. T., Margon, A., Sequi, P., Leita, L. and Legname, G. (2014). Prion protein interaction with soil humic substances: environmental implications. *PLoS ONE* **9**, e100016.

Gottfert, F., Wurm, C. A., Mueller, V., Berning, S., Cordes, V. C., Honigmann, A. and Hell, S. W. (2013). Coaligned dual-channel STED nanoscopy and molecular diffusion analysis at 20 nm resolution. *Biophys. J.* **105**, L01-L03.

Hajj, G. N. M., Lopes, M. H., Mercadante, A. F., Veiga, S. S., da Silveira, R. B., Santos, T. G., Ribeiro, K. C. B., Juliano, M. A., Jacchieri, S. G., Zanata, S. M. et al. (2007). Cellular prion protein interaction with vitronectin supports axonal growth and is compensated by integrins. *J. Cell Sci.* **120**, 1915-1926.

Harris, D. A., Huber, M. T., van Dijken, P., Shyng, S. L., Chait, B. T. and Wang, R. (1993). Processing of a cellular prion protein: identification of N- and C-terminal cleavage sites. *Biochemistry* **32**, 1009-1016.

Hornemann, S., Schorn, C. and Wüthrich, K. (2004). NMR structure of the bovine prion protein isolated from healthy calf brains. *EMBO Rep.* **5**, 1159-1164.

Hub, H. H., Zimmermann, U. and Ringsdorf, H. (1982). Preparation of large unilamellar vesicles. *FEBS Lett.* **140**, 254-256.

Kanaani, J., Prusiner, S. B., Diacovo, J., Baekkeskov, S. and Legname, G. (2005). Recombinant prion protein induces rapid polarization and development of synapses in embryonic rat hippocampal neurons in vitro. *J. Neurochem.* **95**, 1373-1386.

Klar, T. A., Jakobs, S., Dyba, M., Egner, A. and Hell, S. W. (2000). Fluorescence microscopy with diffraction resolution barrier broken by stimulated emission. *Proc. Natl. Acad. Sci. USA* **97**, 8206-8210.

Kolodkin, A. L. and Tessier-Lavigne, M. (2011). Mechanisms and molecules of neuronal wiring: a primer. *Cold Spring Harb. Perspect. Biol.* **3**, a001727.

Lauren, J., Gimbel, D. A., Nygaard, H. B., Gilbert, J. W. and Strittmatter, S. M. (2009). Cellular prion protein mediates impairment of synaptic plasticity by amyloid-beta oligomers. *Nature* **457**, 1128-1132.

Li, Y., Jia, Y.-C., Cui, K., Li, N., Zheng, Z.-Y., Wang, Y.-Z. and Yuan, X.-B. (2005). Essential role of TRPC channels in the guidance of nerve growth cones by brain-derived neurotrophic factor. *Nature* **434**, 894-898.

Lilien, J. and Balsamo, J. (2005). The regulation of cadherin-mediated adhesion by tyrosine phosphorylation/dephosphorylation of beta-catenin. *Curr. Opin. Cell Biol.* **17**, 459-465.

Linden, R., Martins, V. R., Prado, M. A. M., Cammarota, M., Izquierdo, I. and Brentani, R. R. (2008). Physiology of the prion protein. *Physiol. Rev.* **88**, 673-728.

Loubet, D., Dakowski, C., Pietri, M., Pradines, E., Bernard, S., Callebert, J., Ardila-Osorio, H., Mouillet-Richard, S., Launay, J.-M., Kellermann, O. et al. (2012). Neuritogenesis: the prion protein controls beta1 integrin signaling activity. *FASEB J.* **26**, 678-690.

Malaga-Trillo, E., Solis, G. P., Schrock, Y., Geiss, C., Luncz, L., Thomanetz, V. and Stuermer, C. A. O. (2009). Regulation of embryonic cell adhesion by the prion protein. *PLoS Biol.* **7**, e1000055.

Martins, V. R., Beraldo, F. H., Hajj, G. N., Lopes, M. H., Lee, K. S., Prado, M. A. and Linden, R. (2010). Prion protein: orchestrating neurotrophic activities. *Curr. Issues Mol. Biol.* **12**, 63-86.

McDonald, A. J. and Millhauser, G. L. (2014). PrP overdrive: does inhibition of alpha-cleavage contribute to PrP(C) toxicity and prion disease? *Prion* **8**, 183-191.

Moore, S. W., Tessier-Lavigne, M. and Kennedy, T. E. (2007). Netrins and their receptors. *Adv. Exp. Med. Biol.* **621**, 17-31.

Ochs, K. and Málaga-Trillo, E. (2014). Common themes in PrP signaling: the Src remains the same. *Front. Cell Dev. Biol.* **2**, 63.

Parkin, E. T., Watt, N. T., Turner, A. J. and Hooper, N. M. (2004). Dual mechanisms for shedding of the cellular prion protein. *J. Biol. Chem.* **279**, 11170-11178.

Perrier, V., Solassol, J., Crozet, C., Frobert, Y., Mourton-Gilles, C., Grassi, J. and Lehmann, S. (2004). Anti-PrP antibodies block PrPSc replication in prion-infected cell cultures by accelerating PrPC degradation. *J. Neurochem.* **89**, 454-463.

Petsch, B., Muller-Schiffmann, A., Lehle, A., Zirdum, E., Prikulis, I., Kuhn, F., Raeber, A. J., Ironside, J. W., Korth, C. and Stitz, L. (2011). Biological effects and use of PrPSc- and PrP-specific antibodies generated by immunization with purified full-length native mouse prions. *J. Virol.* **85**, 4538-4546.

Pinato, G., Raffaelli, T., D'Este, E., Tavano, F. and Cojoc, D. (2011). Optical delivery of liposome encapsulated chemical stimuli to neuronal cells. *J. Biomed. Optics* **16**, 095001.

Pinato, G., Cojoc, D., Lien, L. T., Ansuini, A., Ban, J., D'Este, E. and Torre, V. (2012). Less than 5 Netrin-1 molecules initiate attraction but 200 Sema3A molecules are necessary for repulsion. *Sci. Rep.* **2**, 675.

Premzl, M., Sangiorgio, L., Strumbo, B., Marshall Graves, J. A., Simonic, T. and Gready, J. E. (2003). Shadoo, a new protein highly conserved from fish to mammals and with similarity to prion protein. *Gene* **314**, 89-102.

Prusiner, S. B., Scott, M. R., DeArmond, S. J. and Cohen, F. E. (1998). Prion protein biology. *Cell* **93**, 337-348.

Pushie, M. J., Pickering, I. J., Martin, G. R., Tsutsui, S., Jirik, F. R. and George, G. N. (2011). Prion protein expression level alters regional copper, iron and zinc content in the mouse brain. *Metallomics* **3**, 206-214.

Redecke, L., Binder, S., Elmallah, M. I. Y., Broadbent, R., Tilkorn, C., Schulz, B., May, P., Goos, A., Eich, A., Rübhausen, M. et al. (2009). UV-light-induced conversion and aggregation of prion proteins. *Free Radic. Biol. Med.* **46**, 1353-1361.

Santuccione, A., Sytnyk, V., Leshchyns'ka, I. and Schachner, M. (2005). Prion protein recruits its neuronal receptor NCAM to lipid rafts to activate p59fyn and to enhance neurite outgrowth. *J. Cell Biol.* **169**, 341-354.

Schmitt-Ulms, G., Legname, G., Baldwin, M. A., Ball, H. L., Bradon, N., Bosque, P. J., Crossin, K. L., Edelman, G. M., DeArmond, S. J., Cohen, F. E. et al. (2001). Binding of neural cell adhesion molecules (N-CAMs) to the cellular prion protein. *J. Mol. Biol.* **314**, 1209-1225.

Schrock, Y., Solis, G. P. and Stuermer, C. A. O. (2009). Regulation of focal adhesion formation and filopodia extension by the cellular prion protein (PrPC). *FEBS Lett.* **583**, 389-393.

Snajder, M., Vilfan, T., Cernilec, M., Rupreht, R., Popovic, M., Juntes, P., Serbec, V. C. and Ulrih, N. P. (2012). Enzymatic degradation of PrPSc by a protease secreted from Aeropyrum pernix K1. *PLoS ONE* **7**, e39548.

Spevacek, A. R., Evans, E. G. B., Miller, J. L., Meyer, H. C., Pelton, J. G. and Millhauser, G. L. (2013). Zinc drives a tertiary fold in the prion protein with familial disease mutation sites at the interface. *Structure* **21**, 236-246.

Steele, A. D., Emsley, J. G., Ozdinler, P. H., Lindquist, S. and Macklis, J. D. (2006). Prion protein (PrPc) positively regulates neural precursor proliferation during developmental and adult mammalian neurogenesis. *Proc. Natl. Acad. Sci. USA* **103**, 3416-3421.

Sun, B. and Chiu, D. T. (2003). Spatially and temporally resolved delivery of stimuli to single cells. *J. Am. Chem. Soc.* **125**, 3702-3703.

Sun, B. and Chiu, D. T. (2005). Determination of the encapsulation efficiency of individual vesicles using single-vesicle photolysis and confocal single-molecule detection. *Anal. Chem.* **77**, 2770-2776.

Thakur, A. K., Srivastava, A. K., Srinivas, V., Chary, K. V. R. and Rao, C. M. (2011). Copper alters aggregation behavior of prion protein and induces novel interactions between its N- and C-terminal regions. *J. Biol. Chem.* **286**, 38533-38545.

van den Ent, F. and Lowe, J. (2006). RF cloning: a restriction-free method for inserting target genes into plasmids. *J. Biochem. Biophys. Methods* **67**, 67-74.

Vitriol, E. A. and Zheng, J. Q. (2012). Growth cone travel in space and time: the cellular ensemble of cytoskeleton, adhesion, and membrane. *Neuron* **73**, 1068-1081.

Zahn, R., Liu, A., Luhrs, T., Riek, R., von Schroetter, C., Lopez Garcia, F., Billeter, M., Calzolai, L., Wider, G. and Wuthrich, K. (2000). NMR solution structure of the human prion protein. *Proc. Natl. Acad. Sci. USA* **97**, 145-150.